Tianjin Daxue Xuebao (Ziran Kexue yu Gongcheng Jishu Ban)/
Journal of Tianjin University Science and Technology
ISSN (Online):0493-2137
E-Publication: Online Open Access
Vol: 59 Issue: 07:2026
DOI: 10.5281/zenodo.21260887

IMMUNOINFORMATICS-GUIDED MULTI-EPITOPE VACCINE CANDIDATE DESIGN AND MHC DOCKING VALIDATION TARGETING THE GLYCOPROTEIN PRECURSOR OF THE NEWLY REPORTED ANDV/Switzerland/Hu-3337/2026 ORTHOHANTAVIRUS

KHALED MATAR
Tun Abdullah Ahmed Badawi Cancer Centre, University of Science Malaysia.

MARYAM ALSENUSSI ALLAFI KHALIFA
Healthcare Services Center, Sabha, Libya.

YAHYA SABER E, MANSOUR ABDULGHANY*
Department of Pharmacology and Toxicology, Faculty of Pharmacy Omar Almuktar University, Albayda-Libya. *Corresponding Author Email: yahya.saber@omu.edu.ly

NAJAT ALBAHLOUL ALMABROUK
Department of Preventive Medicine, Azzaytuna University, Tarhuna, Libya.

RYAD ALATI
Ryas Alari, Department of Pharmacology and Toxicology, Faculty of Pharmacy, Alasmarya Islamic University.

Abstract

The rapid release of viral genomic sequences allows early immunoinformatics screening before experimentally curated antigen information becomes available. In this study, the glycoprotein precursor (GP) of the newly reported ANDV/Switzerland/Hu-3337/2026 orthohantavirus was evaluated as a vaccine-design target using a stepwise workflow that integrated antigenicity prediction, conserved-region screening, transmembrane topology, MHC-I and MHC-II epitope prediction, peptide-construct design, and molecular docking against representative MHC receptors. The full GP sequence was predicted as a probable antigen by VaxiJen with a score of 0.5194. Conserved regions 1-50 and 81-240 were retained as antigenic regions and were located outside the predicted membrane-spanning helices. After filtering by MHC binding score and independent VaxiJen antigenicity, two CTL epitopes (VIYEKTHCV and KVKKTVLCY) and six HTL epitopes were selected. Four multi-epitope constructs (F1-F4) were generated using AAY and GPGPG linkers. Docking showed that F4 had the strongest MHC-I docking score (-226.92), whereas F2 had the strongest MHC-II docking score (-260.14). Residue contact-map analysis further indicated that the strongest complexes were supported by hydrogen bonds, salt bridges, alkyl/aliphatic contacts, and van der Waals interactions. These findings prioritize F2 and F4 as leading candidates for further three-dimensional refinement, molecular dynamics, allergenicity/toxicity filtering, population coverage, and experimental validation.

Keywords: Andes Virus; Orthohantavirus; Glycoprotein Precursor; Immunoinformatics; MHC-I; MHC-II; VaxiJen; HDOCK; Multi-Epitope Vaccine.

1. INTRODUCTION

Hantaviruses are segmented, negative-sense RNA viruses with zoonotic importance because several members can cause severe human disease after spillover from rodent

Tianjin Daxue Xuebao (Ziran Kexue yu Gongcheng Jishu Ban)/
Journal of Tianjin University Science and Technology
ISSN (Online):0493-2137
E-Publication: Online Open Access
Vol: 59 Issue: 07:2026
DOI: 10.5281/zenodo.21260887

reservoirs. The rapid reporting of the ANDV/Switzerland/Hu-3337/2026 sequence through Virological.org created an early opportunity to evaluate vaccine-relevant targets before curated UniProt annotations or experimentally solved structures become available (Laubscher et al., 2026). In this situation, computational immunoinformatics is not a replacement for laboratory validation, but it can provide a rational first map of which regions and epitopes deserve experimental attention.

For vaccine design, the viral glycoprotein precursor is a particularly relevant target because the Gn and Gc envelope glycoproteins form the viral surface machinery responsible for entry, fusion, assembly, and immune recognition. Structural and functional studies have shown that hantavirus Gn/Gc glycoproteins are central to the virion surface lattice and are major targets of neutralizing antibodies (Cifuentes-Munoz et al., 2014; Serris et al., 2020).

In Andes virus specifically, monoclonal antibodies targeting Gn and Gc can neutralize infection and protect in preclinical models, supporting the biological value of glycoprotein-focused antigen discovery (Duehr et al., 2020; Engdahl et al., 2023).

The main gap is that a newly reported sequence cannot be treated as a mature vaccine candidate simply because it encodes a surface protein. A useful design pipeline must connect several pieces of evidence: the protein should be antigenic, the selected regions should be conserved, the epitopes should be accessible rather than buried in transmembrane helices, predicted MHC binders should retain independent antigenicity, and candidate peptide constructs should form reasonable receptor interfaces in docking.

Therefore, this study followed a KSI-style logic: background and gap first, then stepwise computational evidence, then interpretation of how each result contributes to the final vaccine-design decision.

The aim of the study was to identify conserved antigenic GP regions, select high-confidence MHC-I and MHC-II epitopes, assemble them into multi-epitope peptide constructs, and prioritize constructs by docking against representative MHC-I and MHC-II receptors. This design provides a practical starting point for subsequent molecular dynamics, immune simulation, population coverage, and experimental immunogenicity testing.

2. MATERIALS AND METHODS

2.1 Sequence source and glycoprotein target selection

The complete consensus sequence of ANDV/Switzerland/Hu-3337/2026 was obtained from the public Virological.org report describing the Swiss resident 2026 orthohantavirus sequence.

The M segment-derived glycoprotein precursor was selected for vaccine analysis because envelope glycoproteins are directly relevant to viral entry and immune recognition. The final analyzed GP sequence consisted of 1138 amino acids (Laubscher et al., 2026).

Tianjin Daxue Xuebao (Ziran Kexue yu Gongcheng Jishu Ban)/
Journal of Tianjin University Science and Technology
ISSN (Online):0493-2137
E-Publication: Online Open Access
Vol: 59 Issue: 07:2026
DOI: 10.5281/zenodo.21260887

2.2 Preliminary annotation and manual validation

Initial ORF annotation was performed using Prokka as a preliminary annotation step. Because Prokka is primarily optimized for prokaryotic genome annotation, the output was manually validated according to the canonical orthohantavirus segment products: L segment as RNA-dependent RNA polymerase, M segment as glycoprotein precursor, and S segment as nucleoprotein. This step ensured that the vaccine analysis was performed on the expected M segment product and avoided relying on automated annotation alone (Seemann, 2014).

2.3 Full-length antigenicity prediction

The complete GP amino acid sequence was evaluated using VaxiJen v2.0 under the viral antigen model. VaxiJen is an alignment-independent antigenicity prediction method based on physicochemical properties and is widely used for protective antigen screening (Doytchinova & Flower, 2007). A threshold of 0.4 was used to classify probable antigens.

2.4 Conserved-region detection and region-level antigenicity screening

Multiple sequence alignment was performed to identify conserved regions within the GP sequence. Conserved regions were then independently screened using VaxiJen to determine whether sequence conservation was accompanied by antigenic potential. This two-layer selection strategy was used because conserved but non-antigenic regions may be less useful for vaccine design, while antigenic but poorly conserved regions may provide narrower coverage. The alignment step followed the principle of constraint-based multiple sequence comparison, consistent with COBALT-like approaches (Papadopoulos & Agarwala, 2007).

2.5 Transmembrane topology prediction

GP topology was predicted using TMHMM 2.0 to classify outside, inside, and transmembrane-helix regions. This was necessary because transmembrane helices are generally less suitable as direct peptide vaccine regions than accessible outside segments. TMHMM applies a hidden Markov model to predict transmembrane protein topology and membrane-spanning helices (Krogh et al., 2001).

2.6 MHC-I and MHC-II epitope prediction

The two conserved antigenic regions with the highest VaxiJen scores were submitted to IEDB MHC-I and MHC-II prediction resources. IEDB analysis tools provide standardized resources for immune epitope prediction and prioritization (Dhanda et al., 2019). MHC-I prediction was used to identify candidate cytotoxic T lymphocyte epitopes, whereas MHC-II prediction was used to identify helper T-cell epitopes. The prediction framework is consistent with NetMHCpan/NetMHCIIpan-based peptide-MHC binding prediction (Reynisson et al., 2020).

2.7 Epitope filtering and VaxiJen confirmation

Predicted epitopes were filtered using a binding-score cutoff greater than 0.5. Each retained peptide was then independently evaluated using VaxiJen. For final selection,

Tianjin Daxue Xuebao (Ziran Kexue yu Gongcheng Jishu Ban)/
Journal of Tianjin University Science and Technology
ISSN (Online):0493-2137
E-Publication: Online Open Access
Vol: 59 Issue: 07:2026
DOI: 10.5281/zenodo.21260887

peptides had to satisfy two conditions: binding score greater than 0.5 and VaxiJen score greater than 0.4. This dual-filtering step was applied to avoid retaining strong predicted MHC binders that were not antigenic as independent peptide candidates.

2.8 Peptide construct design and structural modelling

Final MHC-I and MHC-II epitopes were assembled into peptide constructs for downstream modelling and docking. AAY linkers were used between CTL epitopes to support proteasomal processing, while GPGPG linkers were used between CTL and HTL blocks and between HTL epitopes to maintain epitope separation and flexibility. Four final constructs (F1-F4) were selected for receptor docking. Three-dimensional models were generated before docking, consistent with the use of AlphaFold3 or peptide-modelling tools for biomolecular structure prediction (Abramson et al., 2024).

2.9 Molecular docking and residue contact analysis

Protein-peptide docking was performed using HDOCK against representative MHC-I and MHC-II structures. The MHC-I receptor was represented by P04439 and the MHC-II receptor by P01903. HDOCK was selected because it supports integrated template-based and template-free protein-protein docking and is widely used for modelling biomolecular complexes (Yan et al., 2020). Docking scores were recorded for F1-F4 against MHC-I and MHC-II. For the best-performing constructs, residue-residue contacts were analyzed and summarized by interaction type, number of atomic contacts, minimum distance, and interface residues. Contact maps were generated to visualize receptor-side and construct-side interaction hotspots.

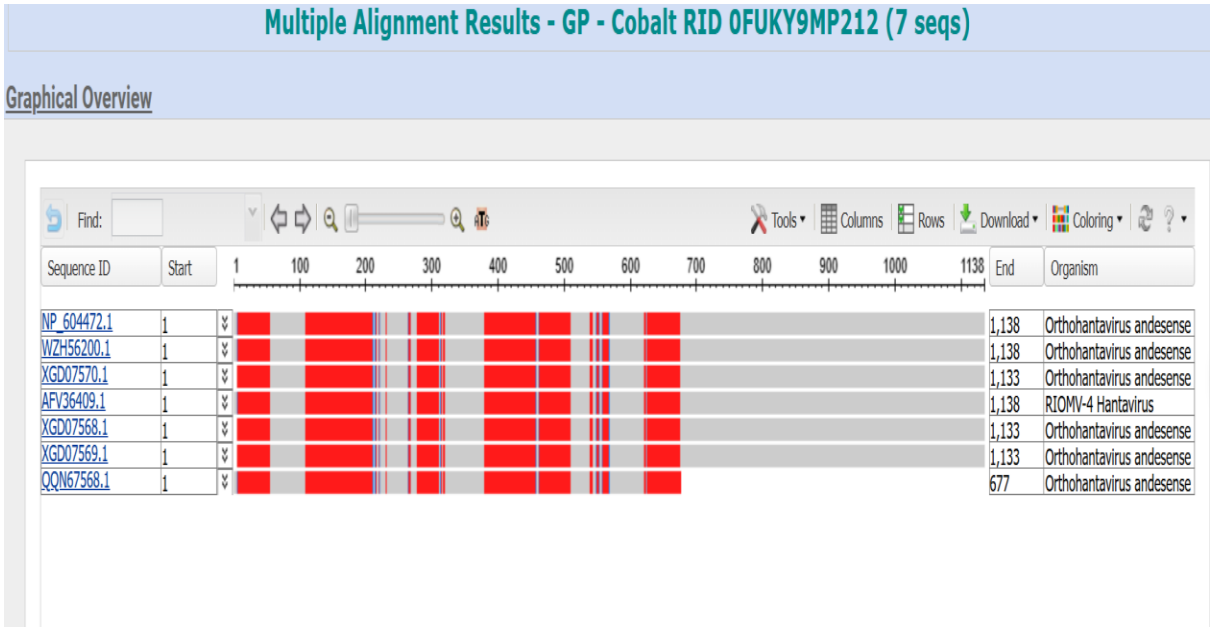

Figure 1: Multiple sequence alignment output used to support conserved-region selection in the GP sequence

Tianjin Daxue Xuebao (Ziran Kexue yu Gongcheng Jishu Ban)/
Journal of Tianjin University Science and Technology
ISSN (Online):0493-2137
E-Publication: Online Open Access
Vol: 59 Issue: 07:2026
DOI: 10.5281/zenodo.21260887

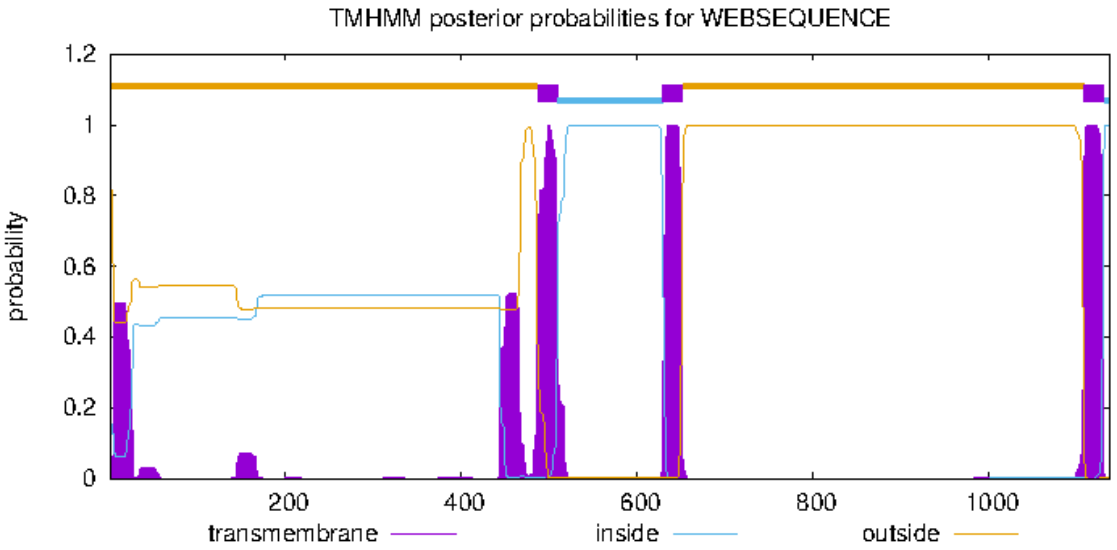

Figure 2: TMHMM 2.0 topology output showing predicted outside, inside, and transmembrane regions of GP

3. RESULTS

3.1 Full GP antigenicity supports vaccine-target selection

The full-length GP sequence produced a VaxiJen score of 0.5194, classifying it as a probable antigen. This result supported continuing the workflow using GP rather than excluding it at the whole-protein stage.

Parameter	Result
Protein target	Glycoprotein precursor (GP)
Protein length	1138 amino acids
Overall VaxiJen score	0.5194
Prediction	Probable antigen
Interpretation	Suitable for downstream immunoinformatics screening

3.2 Conserved-region antigenicity narrows the vaccine search space

Five conserved regions were evaluated by VaxiJen. Only regions 1-50 and 81-240 exceeded the antigenicity threshold, with scores of 0.8855 and 0.5335, respectively. These two regions were retained for MHC-I and MHC-II epitope prediction.

Region	Sequence	VaxiJen	Prediction	Decision
Jan-50	LVVLGVCYTLTLAMPKTIYELKMECPHTVGLGQGYII GSTELGLISIEAA	0.8855	Probable antigen	Selected
81-240	LRGTCILAPELYDTLKKVKKTVLCYDLTCNQTHCQP TVYLIAPVLTCMSIRSCMASVFTSRIQVIYEKTHCVT GQLIEGQCFNPAHTLTLSQPAHTYDTVTLP	0.5335	Probable antigen	Selected
321-480	TVFCTLAGPGASCEAYSENGIFNISSPTCLVNKVQR FRGSEQKINFICQRVDQDVVVYCNGQKKVILTKTLV IGQCIYT	0.1669	Probable non-antigen	Excluded

Tianjin Daxue Xuebao (Ziran Kexue yu Gongcheng Jishu Ban)/
Journal of Tianjin University Science and Technology
ISSN (Online):0493-2137
E-Publication: Online Open Access
Vol: 59 Issue: 07:2026
DOI: 10.5281/zenodo.21260887

401-480	FSLMPDVAHSLAVELCVPGLHGWATVMLLSTFCFG WVLIPAVTLIILKC	0.3961	Probable non-antigen	Excluded
561-641	SRCYVGLVWCLLLTCEIVIWAASAETPLMESGWSD TAHGVGEIPMKTDLE	0.3427	Probable non-antigen	Excluded

3.3 Topology confirms that the selected epitopes are outside the membrane helices

TMHMM predicted a large outside region from positions 1 to 486, followed by transmembrane helices at positions 487-509, 629-651, and 1108-1130. Both selected antigenic conserved regions, 1-50 and 81-240, fall within the outside 1-486 region. This strengthens their relevance for vaccine design because they are not located within predicted transmembrane helices.

Topology	Start	End
Outside	1	486
TM helix	487	509
Inside	510	628
TM helix	629	651
Outside	652	1107
TM helix	1108	1130
Inside	1131	1138

3.4 MHC-I filtering identifies two antigenic CTL epitopes

Seven MHC-I peptides showed prediction scores greater than 0.5. After applying the VaxiJen antigenicity filter, only VIYEKTHCV and KVKKTVLCY remained as final CTL candidates. This filtering step was critical because several strong predicted binders had negative or sub-threshold antigenicity values.

Peptide	MHC-I score	VaxiJen	Prediction	Decision
FTSRIQVIY	0.866679	0.3980	Probable non-antigen	Excluded
VIYEKTHCV	0.935673	1.1203	Probable antigen	Selected
KVKKTVLCY	0.862247	1.1524	Probable antigen	Selected
TLSQPAHTY	0.931620	-0.3547	Probable non-antigen	Excluded
ELYDTLKKV	0.894751	-0.1383	Probable non-antigen	Excluded
SVFTSRIQV	0.837666	0.2694	Probable non-antigen	Excluded
LTLSQPAHTY	0.792659	-0.0244	Probable non-antigen	Excluded

3.5 MHC-II filtering identifies six antigenic HTL epitopes

Seven MHC-II peptides exceeded the binding-score cutoff. Six peptides were antigenic by VaxiJen and were retained. GQCFNPAHTLTLSQP had the highest MHC-II score (0.8934), whereas IEGQCFNPAHTLTLS had the highest VaxiJen score among selected HTL epitopes (1.0193).

Peptide	MHC-II score	VaxiJen	Prediction	Decision
GQCFNPAHTLTLSQP	0.8934	0.5103	Probable antigen	Selected
EGQCFNPAHTLTLSQ	0.8358	0.8767	Probable antigen	Selected
IEGQCFNPAHTLTLS	0.7390	1.0193	Probable antigen	Selected
GQGYIIGSTELGLIS	0.8011	0.7991	Probable antigen	Selected
LGQGYIIGSTELGLI	0.7346	0.8737	Probable antigen	Selected

Tianjin Daxue Xuebao (Ziran Kexue yu Gongcheng Jishu Ban)/
Journal of Tianjin University Science and Technology
ISSN (Online):0493-2137
E-Publication: Online Open Access
Vol: 59 Issue: 07:2026
DOI: 10.5281/zenodo.21260887

Peptide	MHC-II score	VaxiJen	Prediction	Decision
GLGQGYIIGSTELGL	0.6675	0.8589	Probable antigen	Selected
APELYDTLKKVKKTV	0.5655	0.2055	Probable non-antigen	Excluded

3.6 Final selected epitopes

Code	Type	Peptide	Binding score	VaxiJen	Use
CTL1	MHC-I / CTL	VIYEKTHCV	0.935673	1.1203	Selected for CTL arm
CTL2	MHC-I / CTL	KVKKTVLCY	0.862247	1.1524	Selected for CTL arm
HTL1	MHC-II / HTL	GQCFNPAHTLTLSQP	0.8934	0.5103	Selected for HTL arm
HTL2	MHC-II / HTL	EGQCFNPAHTLTLSQ	0.8358	0.8767	Selected for HTL arm
HTL3	MHC-II / HTL	IEGQCFNPAHTLTLS	0.7390	1.0193	Selected for HTL arm
HTL4	MHC-II / HTL	GQGYIIGSTELGLIS	0.8011	0.7991	Selected for HTL arm
HTL5	MHC-II / HTL	LGQGYIIGSTELGLI	0.7346	0.8737	Selected for HTL arm
HTL6	MHC-II / HTL	GLGQGYIIGSTELGL	0.6675	0.8589	Selected for HTL arm

3.7 Peptide construct library and docking-priority constructs

Four representative multi-epitope constructs were selected for docking after arranging the strongest CTL and HTL candidates using AAY and GPGPG linkers. These constructs were designed to compare balanced, high-score, high-antigenicity, and shorter peptide architectures.

ID	Construct sequence
F1	VIYEKTHCV-AAY-KVKKTVLCY-GPGPG-GQCFNPAHTLTLSQP-GPGPG-EGQCFNPAHTLTLSQ
F2	VIYEKTHCV-AAY-KVKKTVLCY-GPGPG-GQCFNPAHTLTLSQP-GPGPG-IEGQCFNPAHTLTLS
F3	VIYEKTHCV-AAY-KVKKTVLCY-GPGPG-GQCFNPAHTLTLSQP-GPGPG-GQGYIIGSTELGLIS
F4	VIYEKTHCV-AAY-KVKKTVLCY-GPGPG-GQCFNPAHTLTLSQP-GPGPG-LGQGYIIGSTELGLI

3.8 Docking scores against MHC-I and MHC-II

Docking was performed against MHC-I (P04439) and MHC-II (P01903). F4 showed the strongest MHC-I docking score, while F2 showed the strongest MHC-II docking score. This means that the best construct depends on the receptor arm considered: F4 is favored for MHC-I interaction, whereas F2 is favored for MHC-II interaction.

Construct	Sequence	MHC-I docking score	MHC-II docking score	Interpretation
F1	VIYEKTHCV-AAY-KVKKTVLCY-GPGPG-GQCFNPAHTLTLSQP-GPGPG-EGQCFNPAHTLTLSQ	-187.81	-219.45	Balanced construct with top two HTL cluster peptides
F2	VIYEKTHCV-AAY-KVKKTVLCY-GPGPG-GQCFNPAHTLTLSQP-GPGPG-IEGQCFNPAHTLTLS	-176.52	-260.14	Best MHC-II docking score; includes the top MHC-II score peptide and the highest VaxiJen HTL peptide

Tianjin Daxue Xuebao (Ziran Kexue yu Gongcheng Jishu Ban)/
Journal of Tianjin University Science and Technology
ISSN (Online):0493-2137
E-Publication: Online Open Access
Vol: 59 Issue: 07:2026
DOI: 10.5281/zenodo.21260887

Construct	Sequence	MHC-I docking score	MHC-II docking score	Interpretation
F3	VIYEKTHCV-AAY-KVKKTVLCY-GPGPG-GQCFNPAHTLTLSQP-GPGPG-GQGYIIGSTELGLIS	-184.76	-234.27	Includes second antigenic MHC-II hotspot
F4	VIYEKTHCV-AAY-KVKKTVLCY-GPGPG-GQCFNPAHTLTLSQP-GPGPG-LGQGYIIGSTELGLI	-226.92	-246.50	Best MHC-I docking score and second-best MHC-II docking score

3.9 Interface contact summary for F2 and F4 complexes

Residue contact analysis showed that all four analyzed complexes formed multi-residue interfaces. F2-MHC-II showed the highest total number of atomic contacts, whereas F4-MHC-I combined the best MHC-I docking score with a mixed interface containing hydrogen bonding, one salt bridge, aliphatic contacts, and van der Waals contacts.

Complex	Residue-pair contacts	Total atomic contacts	Mean contacts/pair	Minimum distance (A)	H bonds	Salt bridges	Hydrophobic	Alkyl/ aliphatic	Van der Waals
F2-MHC-I	63	538	8.5	1.57	11	1	0	35	16
F2-MHC-II	52	580	11.2	1.44	7	1	0	33	11
F4-MHC-I	60	542	9	2.2	10	1	0	35	14
F4-MHC-II	54	474	8.8	1.4	5	0	1	35	13

3.10 Dominant interface contacts

Complex	MHC residue	Construct residue	Min distance (A)	Atomic contacts	Interaction type
F2-MHC-I	ASN90	PRO41	2.55	38	Alkyl/Aliphatic
F2-MHC-I	TRP191	PRO43	2.23	31	Hydrogen Bond
F2-MHC-I	GLU176	THR37	1.57	28	Hydrogen Bond
F2-MHC-I	GLU178	HIS7	2.99	26	Hydrogen Bond
F2-MHC-I	GLN94	GLN40	1.83	25	Hydrogen Bond
F2-MHC-II	ILE32	ASN53	2.77	42	Alkyl/Aliphatic
F2-MHC-II	PHE51	PHE30	3.35	38	Alkyl/Aliphatic
F2-MHC-II	PHE79	HIS34	2.32	35	Alkyl/Aliphatic
F2-MHC-II	PHE76	TYR3	2.27	32	Alkyl/Aliphatic
F2-MHC-II	PHE76	LYS5	3.15	32	Hydrogen Bond
F4-MHC-I	THR97	LYS15	2.39	27	Hydrogen Bond
F4-MHC-I	THR187	TYR21	3.01	25	Hydrogen Bond
F4-MHC-I	LYS170	TYR12	2.75	20	Alkyl/Aliphatic
F4-MHC-I	ALA93	LYS15	3.16	20	Alkyl/Aliphatic
F4-MHC-I	TRP191	TYR21	3.22	20	Alkyl/Aliphatic
F4-MHC-II	HIS30	LEU19	2.61	31	Hydrogen Bond
F4-MHC-II	PHE51	LYS16	2.36	25	Alkyl/Aliphatic
F4-MHC-II	PHE57	PHE31	2.96	21	Alkyl/Aliphatic
F4-MHC-II	PHE51	VAL18	2.34	20	Alkyl/Aliphatic
F4-MHC-II	PHE76	HIS35	2.76	20	Alkyl/Aliphatic

Tianjin Daxue Xuebao (Ziran Kexue yu Gongcheng Jishu Ban)/
Journal of Tianjin University Science and Technology
ISSN (Online):0493-2137
E-Publication: Online Open Access
Vol: 59 Issue: 07:2026
DOI: 10.5281/zenodo.21260887

3.11 Docked complex views and contact maps

The representative docked complex views and contact maps highlight that the interaction interfaces are not dependent on a single contact. Instead, each complex is supported by distributed residue contacts involving polar, charged, hydrophobic, and van der Waals interactions.

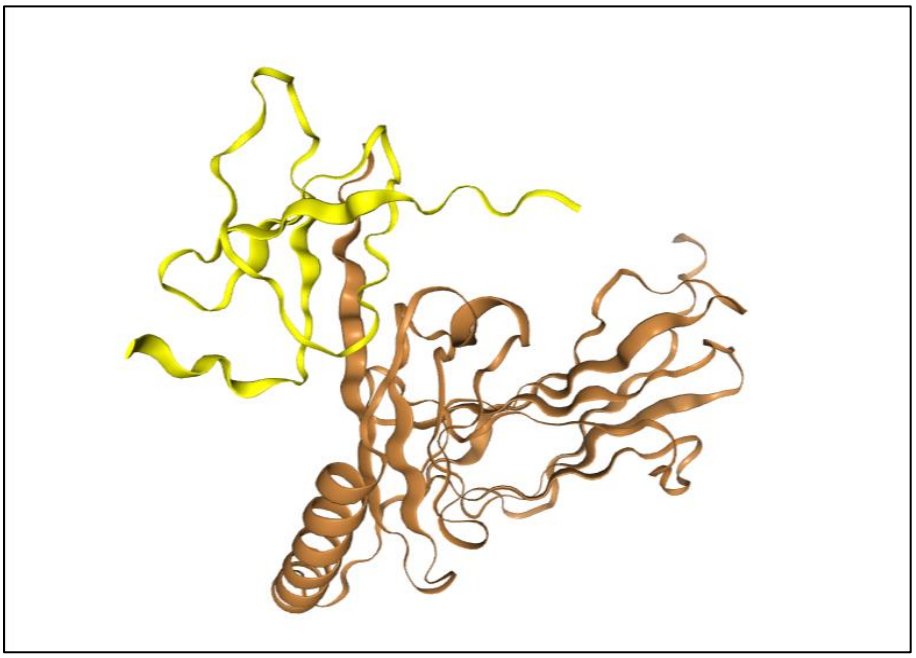

Figure 3: Representative docked complex view of F2 with MHC-II

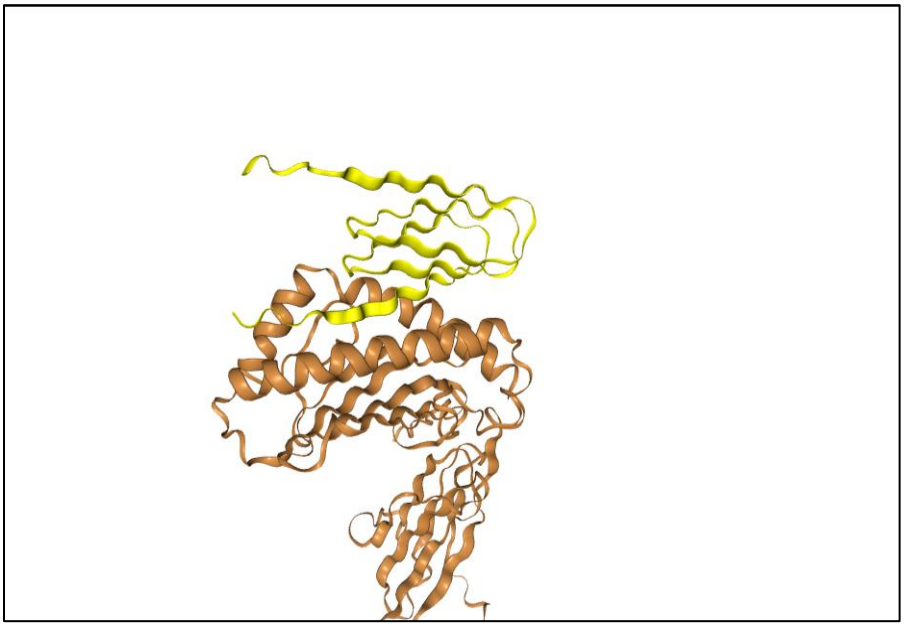

Figure 4: Representative docked complex view of F4 with MHC-I

Tianjin Daxue Xuebao (Ziran Kexue yu Gongcheng Jishu Ban)/
Journal of Tianjin University Science and Technology
ISSN (Online):0493-2137
E-Publication: Online Open Access
Vol: 59 Issue: 07:2026
DOI: 10.5281/zenodo.21260887

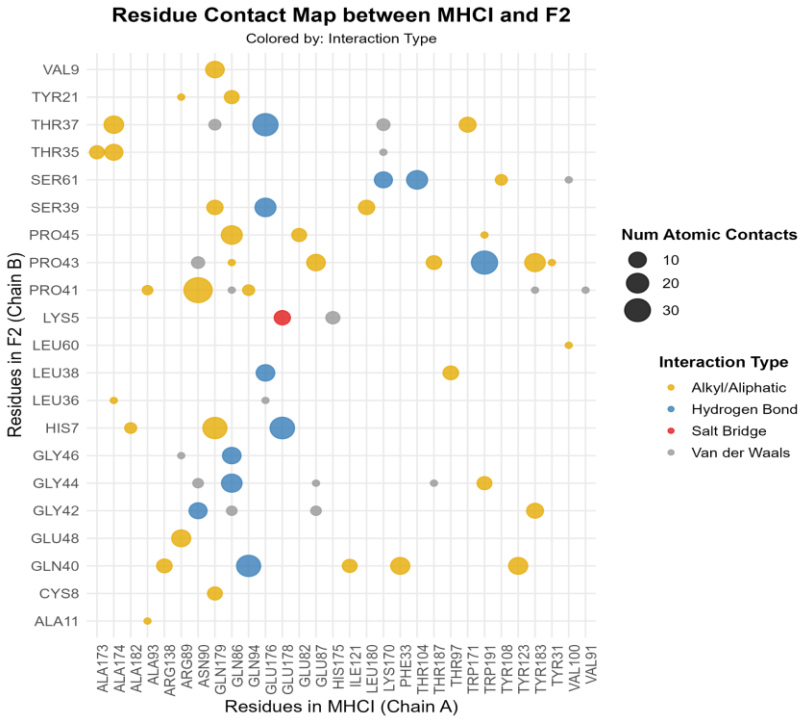

Figure 5: Residue contact map between MHC-I and F2

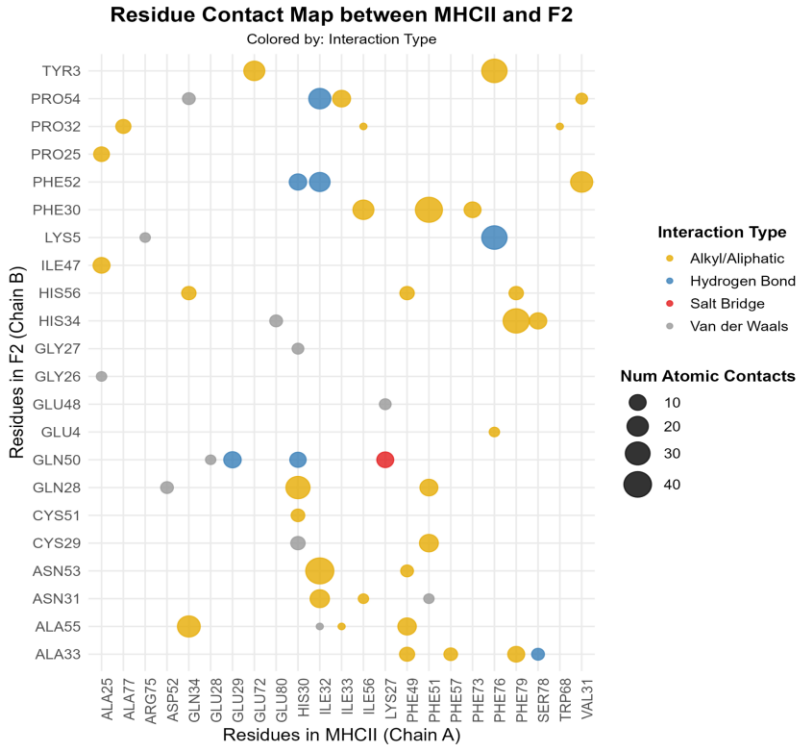

Figure 6: Residue contact map between MHC-II and F2

Tianjin Daxue Xuebao (Ziran Kexue yu Gongcheng Jishu Ban)/
Journal of Tianjin University Science and Technology
ISSN (Online):0493-2137
E-Publication: Online Open Access
Vol: 59 Issue: 07:2026
DOI: 10.5281/zenodo.21260887

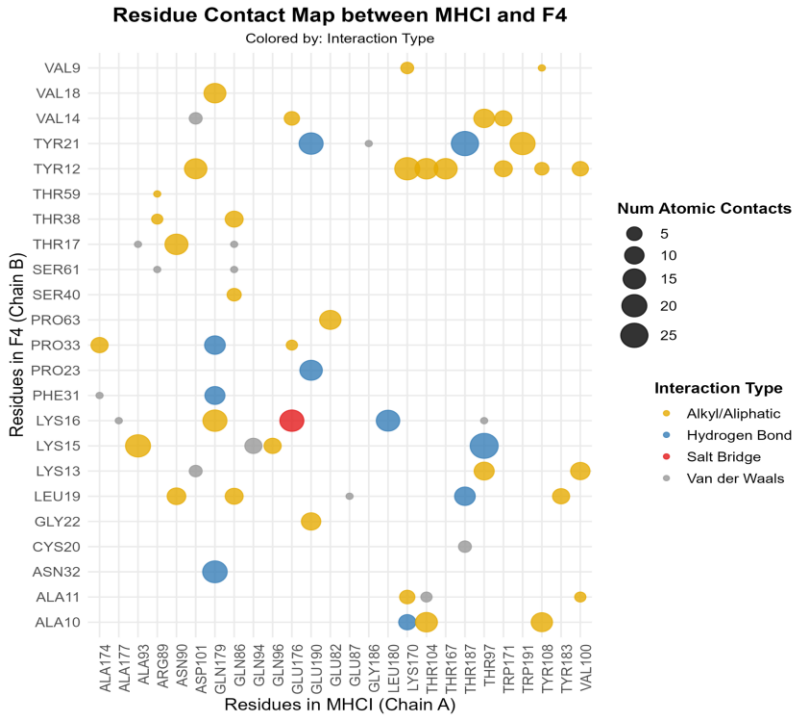

Figure 7: Residue contact map between MHC-I and F4

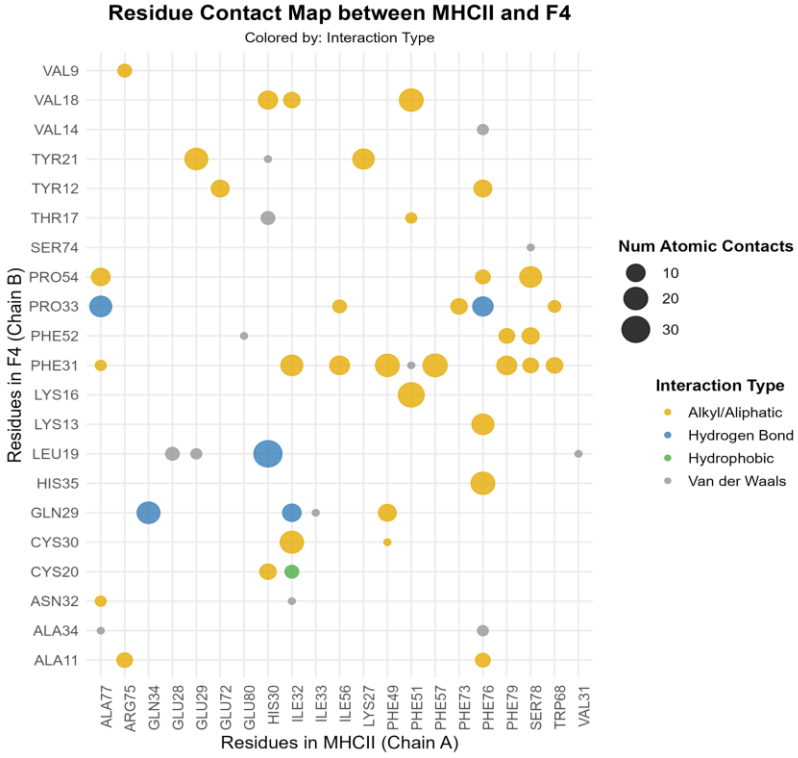

Figure 8: Residue contact map between MHC-II and F4

Tianjin Daxue Xuebao (Ziran Kexue yu Gongcheng Jishu Ban)/
Journal of Tianjin University Science and Technology
ISSN (Online):0493-2137
E-Publication: Online Open Access
Vol: 59 Issue: 07:2026
DOI: 10.5281/zenodo.21260887

4. DISCUSSION

This study used a stepwise immunoinformatics and docking strategy to convert a newly available orthohantavirus GP sequence into a prioritized set of vaccine-relevant peptide candidates. The most important finding is that the GP sequence was not only predicted as antigenic at the full-protein level, but also contained two conserved antigenic regions that were positioned outside predicted membrane helices. This is biologically meaningful because hantavirus Gn and Gc glycoproteins form the exposed viral entry machinery and are central targets of antibody-mediated immune recognition (Cifuentes-Munoz et al., 2014; Serris et al., 2020). Therefore, the selection of GP as the vaccine target aligns with the known role of hantavirus glycoproteins in entry, fusion, and neutralization.

The conserved-region analysis narrowed the target space from the full 1138-amino-acid protein to two antigenic regions, 1-50 and 81-240. This step is important because epitope prediction directly from a complete glycoprotein can produce many candidates that are difficult to justify biologically. Region 1-50 showed the strongest VaxiJen score (0.8855), while region 81-240 was also antigenic and produced multiple strong MHC-I and MHC-II candidates. The fact that these regions were predicted within the outside 1-486 segment supports their relevance, because epitopes located in accessible portions of viral glycoproteins are more plausible immune targets than epitopes buried in transmembrane helices. This agrees with the broader concept that neutralizing immune responses against hantaviruses are mainly directed toward exposed Gn/Gc glycoprotein structures (Duehr et al., 2020; Rissanen et al., 2020).

The MHC-I analysis showed that predicted binding strength alone was not sufficient for candidate selection. Several peptides had MHC-I scores greater than 0.5, but only VIYEKTHCV and KVKKTVLCY remained after independent antigenicity filtering. This dual-filter result is important because a strong predicted binder may still be a weak vaccine candidate if it lacks antigenic potential. VIYEKTHCV had the highest MHC-I score (0.935673), whereas KVKKTVLCY had the highest VaxiJen value among the CTL candidates (1.1524). Together, they provide a logical CTL pair, combining predicted MHC-I presentation with independent antigenicity.

The MHC-II analysis produced a broader HTL set. Six peptides passed both binding-score and VaxiJen filters, with GQCFNPAHTLTLSQP showing the highest MHC-II score (0.8934) and IEGQCFNPAHTLTLS showing the highest VaxiJen score (1.0193). These results suggest that the 77-94 neighborhood around the FNPAHTLTL core is a strong helper T-cell hotspot, while the GQGYIIGSTELGLIS/LGQGYIIGSTELGLI/GLGQGYIIGSTELGL group adds an additional antigenic HTL region. In a multi-epitope vaccine, this is useful because helper T-cell epitopes can support cellular immunity and antibody maturation, while CTL epitopes can support cytotoxic responses against infected cells.

The docking results completed the prioritization puzzle. F4 had the strongest MHC-I docking score (-226.92), while F2 had the strongest MHC-II docking score (-260.14). This split is biologically interpretable rather than contradictory: the same construct does not

Tianjin Daxue Xuebao (Ziran Kexue yu Gongcheng Jishu Ban)/
Journal of Tianjin University Science and Technology
ISSN (Online):0493-2137
E-Publication: Online Open Access
Vol: 59 Issue: 07:2026
DOI: 10.5281/zenodo.21260887

have to be optimal for both receptor classes because MHC-I and MHC-II grooves differ in length preference, openness, residue distribution, and peptide accommodation. F4 therefore appears more favorable for the MHC-I arm, whereas F2 appears more favorable for the MHC-II arm. This supports keeping both F2 and F4 as lead constructs rather than selecting only one at this stage.

The contact-map results strengthened the docking interpretation. F4-MHC-I, the strongest MHC-I complex, formed 60 residue-pair contacts and 542 atomic contacts, including hydrogen bonds and a salt bridge between GLU176 and LYS16. Several high-contact hydrogen-bonding pairs, including THR97-LYS15, THR187-TYR21, GLN179-ASN32, and GLU190-TYR21, suggest that the interface is not driven only by nonspecific hydrophobic packing. The presence of a salt bridge is especially relevant because electrostatic interactions can help anchor peptide-receptor complexes and stabilize orientation within the binding interface.

F2-MHC-II, the strongest MHC-II complex, showed 52 residue-pair contacts and the highest total atomic contacts among the analyzed interfaces (580). Its interface was dominated by alkyl/aliphatic interactions, with additional hydrogen bonds and one salt bridge. High-contact pairs such as ILE32-ASN53, PHE51-PHE30, PHE79-HIS34, and PHE76-LYS5 indicate that the complex uses a broad hydrophobic/aromatic contact surface supported by specific polar interactions. This pattern fits the docking score, because strong peptide-MHC binding is often supported by a combination of shape complementarity, hydrophobic packing, and residue-specific hydrogen bonding rather than by a single interaction type.

Comparing F2 and F4 suggests a practical downstream strategy. F2 should be prioritized when the goal is to maximize MHC-II-related helper T-cell presentation, while F4 should be prioritized when the goal is to maximize MHC-I docking behavior. Because multi-epitope vaccine candidates need both CTL and HTL support, the best interpretation is not to discard one construct but to advance F2 and F4 together into molecular dynamics simulation, population coverage analysis, allergenicity/toxicity screening, and immune simulation. This staged approach is consistent with modern computational vaccine-design practice, where epitope prediction, structural modelling, docking, and post-docking validation are integrated rather than treated as isolated scores (Dhanda et al., 2019; Reynisson et al., 2020; Yan et al., 2020).

The study has important limitations. First, all findings are computational and should be considered preliminary until experimentally validated. Second, docking scores from HDOCK are useful for ranking and interface interpretation but should not be treated as experimental binding affinities. Third, the receptor models used here represent selected MHC molecules, and broader HLA population coverage is still needed. Fourth, additional filters such as allergenicity, toxicity, solubility, stability, immune simulation, and molecular dynamics should be added before proposing a final vaccine construct. Despite these limitations, the workflow provides a coherent early-stage design framework for a newly reported sequence and identifies F2 and F4 as the most defensible constructs for the next validation step.

Tianjin Daxue Xuebao (Ziran Kexue yu Gongcheng Jishu Ban)/
Journal of Tianjin University Science and Technology
ISSN (Online):0493-2137
E-Publication: Online Open Access
Vol: 59 Issue: 07:2026
DOI: 10.5281/zenodo.21260887

5. CONCLUSION

The ANDV/Switzerland/Hu-3337/2026 GP sequence was predicted to be a suitable antigenic vaccine target. Conserved antigenic regions 1-50 and 81-240 were located outside predicted membrane helices and generated high-quality MHC-I and MHC-II epitopes after dual filtering. The final CTL candidates were VIYEKTHCV and KVKKTVLCY, while the HTL set was led by GQCFNPAHTLTLSQP and IEGQCFNPAHTLTLS. Docking prioritized F4 for MHC-I interaction and F2 for MHC-II interaction. Therefore, F2 and F4 should be advanced as lead constructs for molecular dynamics, population coverage, immune simulation, allergenicity/toxicity assessment, and eventual experimental validation.

References

1) Abramson, J., Adler, J., Dunger, J., Evans, R., Green, T., Pritzel, A., Ronneberger, O., Willmore, L., Ballard, A. J., Bambrick, J., Bodenstein, S. W., Evans, D. A., Hung, C. C., O'Neill, M., Reiman, D., Tunyasuvunakool, K., Wu, Z., Zemgulyte, A., Arvaniti, E., ... Jumper, J. M. (2024). Accurate structure prediction of biomolecular interactions with AlphaFold 3. Nature, 630, 493-500. https://doi.org/10.1038/s41586-024-07487-w

2) Cifuentes-Munoz, N., Salazar-Quiroz, N., & Tischler, N. D. (2014). Hantavirus Gn and Gc envelope glycoproteins: Key structural units for virus cell entry and virus assembly. Viruses, 6(4), 1801-1822. https://doi.org/10.3390/v6041801

3) Dhanda, S. K., Mahajan, S., Paul, S., Yan, Z., Kim, H., Jespersen, M. C., Jurtz, V., Andreatta, M., Greenbaum, J. A., Marcatili, P., Sette, A., Nielsen, M., & Peters, B. (2019). IEDB-AR: Immune Epitope Database-analysis resource in 2019. Nucleic Acids Research, 47(W1), W502-W506. https://doi.org/10.1093/nar/gkz452

4) Doytchinova, I. A., & Flower, D. R. (2007). VaxiJen: A server for prediction of protective antigens, tumour antigens and subunit vaccines. BMC Bioinformatics, 8, 4. https://doi.org/10.1186/1471-2105-8-4

5) Duehr, J., McMahon, M., Williamson, B., Amanat, F., Durbin, A., Hawman, D. W., Noack, D., Uhl, S., Tan, G. S., Feldmann, H., Krammer, F., & Bukreyev, A. (2020). Neutralizing monoclonal antibodies against the Gn and the Gc of the Andes virus glycoprotein spike complex protect from virus challenge in a preclinical hamster model. mBio, 11(2), e00028-20. https://doi.org/10.1128/mBio.00028-20

6) Engdahl, T. B., Binshtein, E., Nelson, C. A., et al. (2023). Antigenic mapping and functional characterization of human New World hantavirus neutralizing antibodies. eLife, 12, e81743. https://doi.org/10.7554/eLife.81743

7) Krogh, A., Larsson, B., von Heijne, G., & Sonnhammer, E. L. L. (2001). Predicting transmembrane protein topology with a hidden Markov model: Application to complete genomes. Journal of Molecular Biology, 305(3), 567-580. https://doi.org/10.1006/jmbi.2000.4315

8) Laubscher, F., Bloemberg, G., Chudzinski, V., Cordey, S., Huber, M., Perez-Rodriguez, F.-J., Pichler, I., Schibler, M., Thomasson, V., & Ziltener, G. (2026, May 8). Complete sequence of Orthohantavirus andesense virus: Swiss resident 2026. Virological.org. https://virological.org/t/complete-sequence-of-orthohantavirus-andesense-virus-swiss-resident-2026/1023

9) Papadopoulos, J. S., & Agarwala, R. (2007). COBALT: Constraint-based alignment tool for multiple protein sequences. Bioinformatics, 23(9), 1073-1079. https://doi.org/10.1093/bioinformatics/btm076

Tianjin Daxue Xuebao (Ziran Kexue yu Gongcheng Jishu Ban)/
Journal of Tianjin University Science and Technology
ISSN (Online):0493-2137
E-Publication: Online Open Access
Vol: 59 Issue: 07:2026
DOI: 10.5281/zenodo.21260887

10) Reynisson, B., Alvarez, B., Paul, S., Peters, B., & Nielsen, M. (2020). NetMHCpan-4.1 and NetMHCIIpan-4.0: Improved predictions of MHC antigen presentation by concurrent motif deconvolution and integration of MS MHC eluted ligand data. Nucleic Acids Research, 48(W1), W449-W454. https://doi.org/10.1093/nar/gkaa379

11) Rissanen, I., Stass, R., Krumm, S. A., Seow, J., Hulswit, R. J. G., Paesen, G. C., Hepojoki, J., Vapalahti, O., Lundkvist, A., Reynard, O., Volchkov, V., Doores, K. J., Huiskonen, J. T., & Bowden, T. A. (2020). Molecular rationale for antibody-mediated targeting of the hantavirus fusion glycoprotein. eLife, 9, e58242. https://doi.org/10.7554/eLife.58242

12) Seemann, T. (2014). Prokka: Rapid prokaryotic genome annotation. Bioinformatics, 30(14), 2068-2069. https://doi.org/10.1093/bioinformatics/btu153

13) Serris, A., Stass, R., Bignon, E. A., Muena, N. A., Manuguerra, J.-C., Jangra, R. K., Li, S., Chandran, K., Tischler, N. D., Huiskonen, J. T., Rey, F. A., & Guardado-Calvo, P. (2020). The hantavirus surface glycoprotein lattice and its fusion control mechanism. Cell, 183(2), 442-456.e16. https://doi.org/10.1016/j.cell.2020.08.023

14) Yan, Y., Tao, H., He, J., & Huang, S.-Y. (2020). The HDOCK server for integrated protein-protein docking. Nature Protocols, 15(5), 1829-1852. https://doi.org/10.1038/s41596-020-0312-x